Thermochimica Acta, 23 (1978) 171–182

THE THERMAL DECOMPOSITION OF VERMICULITE

P. KRESTEN
Department of Geology, University of Stockholm (Sweden)
G. BERGGREN
AB Atomenergi, Studsvik (Sweden)
(Received 7 March 1977)

ABSTRACT

Vermiculite shows some promising potentials, both as ion-exchange material and thermal insulation. The thermal decomposition of vermiculite from Sokli, Finland, has been studied by various thermoanalytical methods, including high-temperature X-ray diffraction and high-pressure DTA. The major phases occurring during successive heating are: 15Å → 11.8Å → 10.1Å → 9.7Å → 9.3Å (all d_{002} spacings). Reaction enthalpies and activation energies are given for most of the reactions. For the evaluation of kinetic parameters, high-temperature X-ray diffraction is suggested as a powerful tool, superior to most conventional methods.

INTRODUCTION

At the Sokli carbonatite complex in Northern Finland[1, 2], vermiculite occurs both in phosphate rock regoliths and weathered crusts of carbonatite.

To date, the composition of the vermiculite has only been determined by energy dispersive analysis (Geological Survey of Sweden). Of the exchangeable cations, calcium seems to predominate over magnesium; cations in octahedral coordination comprise Mg, Fe, Al and some Ti.

The scope of this study was not only to depict the thermal decomposition of vermiculite from Sokli, adding vermiculite from one more locality to those already investigated by many authors. The intention was also to use a variety of different thermoanalytical methods — some of which have not been employed previously in vermiculite studies — and to interpret the results in terms of reaction kinetics.

EXPERIMENTAL

(a) Samples

For the present study, three specimens have been used:

(1) a large single flake of vermiculite (60×50×20 mm)

(2) as above (40×40×15 mm)

(3) a composite sample of five large flakes.

Specimens Nos 1 and 2 have been filed with a steel file, following the recommendation by Mackenzie[3]. Specimen No. 3 was ground in a Culatti laboratory mill (rotating hammers in a steel cylinder) to less than 150 microns. All specimens were equilibrated under the following conditions:

(1) storage in a desiccator charged with silica gel (relative humidity approaching zero)

(2) storage in a desiccator charged with saturated magnesium nitrate solution[3]. Relative humidity 55%.

(3) storage in distilled water, filtration immediately prior to analysis (relative humidity approaching 100%).

(b) Equipment

The following instruments were used:

(1) Linseis L-62 DTA-equipment (Department of Geology, Stockholm). All samples were run in static air atmosphere, in 0.09 cm^3 alumina crucibles, using alumina as inert material. The thermocouple, Pt-Pt/10%Rh, was calibrated against ICTA reference materials.

(2) Stanton HT thermobalance (Department of Geology, Stockholm). Runs were performed in alumina crucibles in static air atmosphere, at heating rates of 3 and 6°C min^{-1}.

(3) Jeol DX-GO-S diffractometer with high-temperature equipment (Department of Geology, Stockholm). The specimens have been studied at scanning speeds of 1°C (2θ) min^{-1} (static approach) and heating rates of 2.5 and 5°C min^{-1} (dynamic approach). Pt-Pt/13%Rh thermocouples have been used.

(4) Netzsch dilatometer (AB Atomenergi, Studsvik).

(5) Netzsch STA equipment (The University, Bonn, G.F.R.), with simultaneous registration of T, DTA, TG and DTG curves, at a heating rate of 10°C min^{-1}, in Pt crucibles and argon atmosphere (static).

(6) Netzsch 404H high-pressure DTA (The University, Bonn, G.F.R.), using argon as pressure medium, at pressures in the range 5–470 bar.

RESULTS AND DISCUSSION

(a) Scheme of the thermal decomposition

The thermal decomposition of vermiculite can be pictured as follows according to various authors[3–6].

Mg-vermiculite has an initial basal spacing of 14.4–14.8 Å, depending upon the degree of hydration. On heating, it changes to a 13.8Å phase in the range 100–150°C and shortly afterwards to a 11.6–11.8Å phase. The two phases coexist in the range[6] 150–270°C. The structural changes are connected with the loss of four water molecules not in immediate contact with the cation ("unbound water").

With increased temperature, five water molecules not in contact with the cation

in the completely filled single-sheet structure are removed. This is not accompanied by any structural change[5], but is revealed by a strong endothermic DTA effect at about 170°C.

About $2^1/_4$ of the remaining 3 water molecules per cation are released at 270–300°C, accompanied by a structural change from 11.6 to 20.6Å (11.6 ÷ 9.02), according to Walker and Cole[5]. Bobrov et al.[6], however, found a 9.9Å phase in the region 350–700°C, and a 10.5Å phase in the region 270–500°C slowly converting into the 9.9Å phase. They therefore conclude that the 10.5Å phase is "not an individual phase, but a mixture of the 11.6 and 9.9Å components; with an increase in temperature, the amount of the first component decreases" (op. cit., p. 532). Between 650 and 750°C, the remaining water is driven off, accompanied by a structural collapse to 9.02 (or 9.15) Å.

Between 800 and 900°C, the DTA curve shows two endothermic effects which are identified with the stepwise dehydroxylation of the talc-like 9Å phase. In immediate succession, anhydrous mineral assemblages (commonly olivine plus enstatite) are formed.

A number of different temperatures have been selected for X-ray diffraction of specimen No. 3 of vermiculite. The results, Table 1, show fairly good agreement with the literature data quoted above. The larger initial spacing, 15.0Å, is explained by the predominance of calcium as exchangeable cation[7]. In order to establish the temperature ranges during which these phases are stable, the goniometer of the equipment was kept at constant 2θ, while the temperature was raised.

TABLE 1

HIGH-TEMPERATURE X-RAY DIFFRACTION: SOKLI VERMICULITE, SPECIMEN NO. 3

Relative humidity at start: 55%

Temp. (°C)	*I (rel)*	d_{002} *(Å)*
22	100	15.0
100	120	11.9
150	90	11.8
200	20	10.06
250	20	10.06
300	20	10.15
400	20	10.15
500	20	10.15
600	10	9.7
700	10	9.5
800	10	9.3
22 (cooled)	10	9.4

Note: Intensities refer to initial intensity = 100.

The 15.0Å phase was found to be stable from room temperature up to temperatures between 52°C (heating rate 2.5°C min^{-1}) and about 70–75°C (heating rate 5°C min^{-1}). The heating rate employed is thus of importance for the stability range of the 15Å phase, as can be expected. The phase transformation 15Å → 13.8Å → 11.8Å is a consecutive reaction; consequently the existence of the 13.8Å phase is not indicated by "static" high-temperature X-ray diffraction. Although we have not studied short-lived phases such as the 13.8Å phase, indirect proof of its existence is found in Fig. 1, which shows the relative abundances of the various phases. In the DTA and TG methods, this consecutive reaction is displayed as though it were a single-step first-order reaction (Fig. 2). Therefore, a strong endothermic effect is registered on the DTA trace, with T_i = 55°C, T_m = 144°C (at a heating rate of 10°C min^{-1}). The weight loss recorded by TG is 11.9% (Fig. 2). As the weight loss during this first reaction is dependent on the pretreatment of the sample, specimen No. 1 has been pretreated under various conditions of humidity. The weight losses recorded are (Stanton HT balance, 6°C min^{-1}): 9.8% at 0% R.H. (relative humidity), 10.4% at 55% R.H. and 36.5% at 100% R.H.

The first appearance of the 11.8Å phase was registered at 45°C. The maximum amounts of the phases were recorded in the range 90–160°C, and above 195° the phase was no longer present (Fig. 1). Walker and Cole[5] give a stability range of 160–270°C, and Bobrov et al.[6] a range of 150–350°C for the simple 11.8Å phase (up to 500°C for the mixture of 11.8 and 9.9Å phases). Again, the breakdown of the 11.8Å phase proceeds as a consecutive reaction 11.8Å → (20.6 or 10.5Å) → 9.9–10.1Å. In this case also, the reaction appears on DTA and TG as though it were a single-step reaction (Fig. 2): on the DTA, a strong endothermic effect with T_m = 256°C is recorded, accompanied by a weight loss of 4.0%. Data on the kinetics of the reaction,

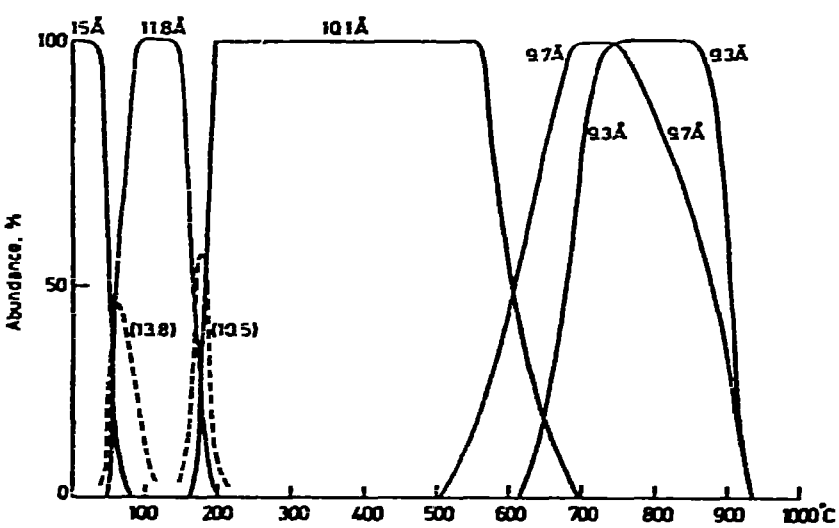

Fig. 1. Scheme of the phases investigated, according to high-temperature X-ray diffraction. Sokli vermiculite, specimen No. 3. Heating rate, 5°C min^{-1}.

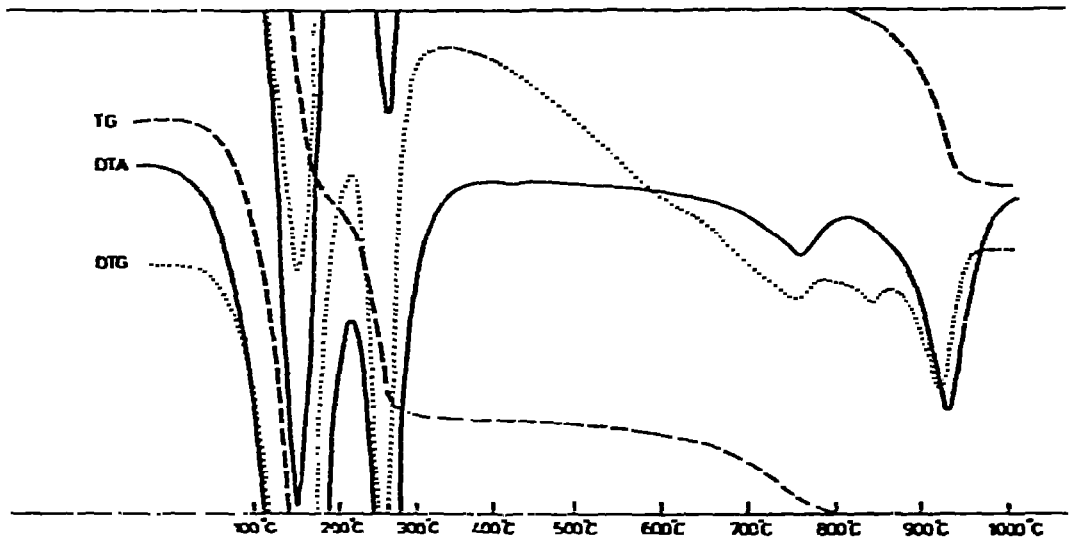

Fig. 2. Simultaneous DTA–TG–DTG of Sokli vermiculite, specimen No. 3, Netzsch STA. 125 mg sample against 125 mg alumina; Pt-crucibles, static argon atmosphere, Pt–Pt/10%Rh thermocouples, heating rate 10 °C min^{-1}. Height of figure corresponds to 0.05 mV on ΔT, 12.5 mg on TG and 0.1 mV ≈ 1.25 mg min^{-1} on DTG.

both stepwise and as a whole, will be discussed below.

The 10.1Å phase forms at about 160° and starts to decompose at about 560°C; the decomposition is completed at about 700°C. Corresponding values are 270–650°C (ref. 5) and 300–700°C (ref. 6). Our present investigation agrees most closely with the one by Bobrov et al., especially with regard to the *d*-spacing. Our data indicate that a slight but continuous loss of weight takes place within the stability range of this phase (Fig. 2), which becomes more marked above 550°C and is there accompanied by an endothermic effect on the DTA (Fig. 2). The breakdown of the 10.1Å phase is revealed by DTA as an endothermic effect, with T_i = 646°C, T_m = 752°C (Fig. 2). The weight loss during this reaction amounts to 1.7%.

The 9.7Å phase appears shortly after 500°C, and is decomposed at 930°C. However, within this range, the 9.7Å phase seems to contract to a 9.3Å phase. This transition seems to proceed continuously, according to high-temperature X-ray diffractograms taken in the "static" manner (Table 1). The "dynamic" approach, however, reveals that the 9.7Å phase starts to decompose at about 710°C, but is present in steadily decreasing amounts up to 930°C (Fig. 1). The 9.3Å phase starts to decompose at 850°C, and is finally decomposed at 930°C. The transition 9.7Å → 9.3Å is revealed by DTA as an endothermic effect preceding the final decomposition and by TG as a loss of weight occurring in two steps. This is most clearly demonstrated by the DTG curve (Fig. 2). The weight losses recorded by TG are 0.6% for 9.7Å → 9.3Å, and 2.7% for 9.3Å → anhydrous.

The final decomposition of vermiculite as a three-step reaction has not been recorded previously. However, the evidence presented here seems conclusive.

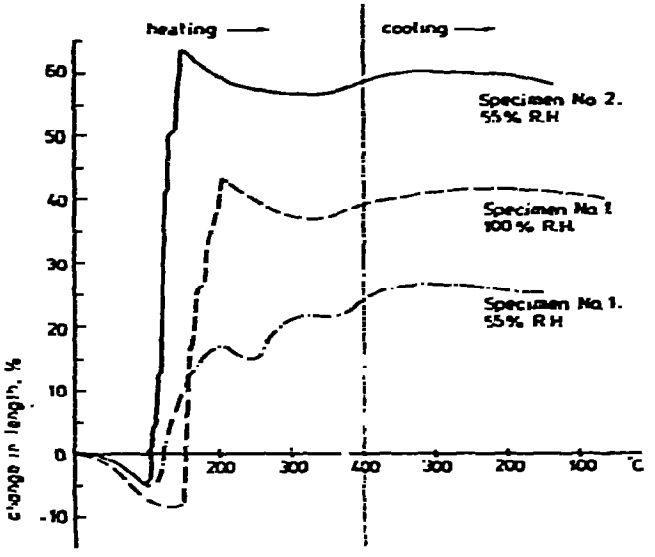

Fig. 3. Dilatometric curves for Sokli vermiculites.

It should also be mentioned that, of all the reactions which occur, only the first one (15Å → 13.8Å → 11.8Å) is reversible. After heating to 80°C (complete breakdown of the 15Å phase), a sample was allowed to cool in the diffractometer. After about 30 min cooling, the vermiculite had recovered to such an extent that the 15Å peak was clearly visible. After an additional 30 min, the intensity of the 15Å peak had reached a level of 40% of the initial intensity.

Sawn pieces of Sokli vermiculite (specimens Nos 1 and 2) have been investigated with the dilatometer. A heating rate of 5°C min^{-1} in air was employed. All length changes refer to changes parallel to the crystallographic *c* axis of the crystals.

During heating, all specimens show an initial contraction, amounting from −5 to −9% (Fig. 3). A more or less rapid expansion follows, amounting from +17 to +63% in the range 150–200°C. Subsequently, a contraction is noted in the range 250–300°C, followed by an increase in length up to 400°C. It is difficult to compare dilatometric curves with the results obtained by other methods. It seems evident, however, that the formation of the 11.8Å phase causes a contraction of the material, while the formation of the 10.1Å phase causes a pronounced expansion.

(b) Evaluation of kinetic parameters

From the DTA trace, Fig. 2, the following values for *n* have been calculated (Table 2) according to the method by Kissinger[9]:

It can thus be stated that the (overall) reaction order of all reactions occurring is $n \approx 1$, as is expected from the reaction types involved (simplified: A → B + C).

In addition, reaction orders have been determined by the method of Gyulai and Greenhow[8], using the TG–DTG traces (Fig. 2). For the reaction 9.7Å → 9.3Å, *n* is unity. In all other cases, *n* was found to be in the range 1/3–4/5, indicating that

TABLE 2

Peak, T_m(°C)	*Reaction*	*n*
144	15Å → 13.8Å → 11.8Å	1.08
256	11.8Å → 10.5Å → 10.1Å	0.93
752	10.1Å → 9.7Å →	0.89
927	9.3Å → anhydrous	0.97

the method is not very useful. Activation energies have been calculated in a number of ways:

(1) From DTA-traces according to Kissinger[9], using heating rates in the range 2–50°C min^{-1} (5 points).

(2) From DTA-traces according to Piloyan[10], using 5–7 points each, at a heating rate of 10°C min^{-1}.

(3) From TG-traces according to Coats and Redfern[11], using 5 points each, at a heating rate of 10°C min^{-1}.

(4) From high-temperature X-ray diffractograms, heating rate 5°C min^{-1}, by the method outlined in the following.

Starting from the rate equation $d\alpha/dt = k(1 - \alpha)^n$, where α denotes the fraction of A decomposed at time t for the reaction $A_{(s)} \rightarrow B_{(s)} + C_{(g)}$, Coats and Redfern[11] devised a method for the calculation of E from TG traces. For first order reactions, they arrived at the conclusion that a plot of $\log [-\log(1 - \alpha)] \cdot T^{-2}$ against $1/T$ will result in a straight line with the slope $-E/2.3R$. Since the intensity recorded on the diffractograms reflects the amounts of phase present at a certain time, the method of Coats and Redfern is directly applicable to dynamic high-temperature X-ray diffraction, if the decomposition of a phase is registered. As a matter of fact, this represents a more direct approach than the use of TG traces (where the amount of A is determined by the amount of C lost). In the case of the formation of a phase, the rate equation can be rewritten as $-d\beta/dt = k\beta^n$, and the Coats-Redfern plot is thus $\log(-\log \beta/T^2)$ versus $1/T$, where β denotes the fraction of B formed at time t.

We are aware that a number of difficulties exist when applying this method:

(1) Underestimation of amounts may occur, owing to the detection limit of the apparatus.

(2) Imperfect orientation of the minerals also causes underestimates.

(3) Mineral orientation may change during the reaction, either stepwise or continuously.

Several of these, and other, difficulties could be overcome by careful calibration work, such as mixing the material with non-reacting material. However, the intention of this paper has not been to present a thorough account of the use of high-temperature X-ray diffraction for the estimation of kinetic parameters. Much more work is required, and we feel that the promising results obtained in this study justify further investigations of this topic.

TABLE 3

ACTIVATION ENERGIES (kcal mol^{-1}) OBTAINED BY VARIOUS METHODS OF CALCULATION

Phases (Å)	*1st*	*2nd*	*3rd*	*4th*	*5th*
	15→13.8→11.8	*11.8→10.5→10.1*	*10.1→9.7*	*9.7→9.3*	*9.3→anhydr*
X-ray diffr formation	— —	— 77.7, 81.6	29.4	56.3	—
X-ray diffr decomposition	— —	50.6 —	30.8	46.5	171.5
DTA (Kissinger)	14	15.5	—	—	—
DTA (Piloyan)	8.5	28.2	22.4	49.3	100.6
TG (Coats & Redfern)	12.4	32.2	43.3	109.8	128.5

Note: The first two reactions cannot be separated by DTA and TG; "bulk values" are given.

The results of all calculations performed have been compiled in Table 3. For the first reaction, no calculations based on X-ray data have been performed, owing to the rather poor temperature control of the apparatus at temperatures below 100°C. The methods based on DTA and TG yield values for the activation energy in the range 8.5 to 14 kcal mol^{-1}. For the second reaction, conventional methods of calculation show values of 15.5, 28.2 and 32.2 kcal mol^{-1}, respectively (Table 3). Calculations based on X-ray data give values of about 51 kcal mol^{-1} for the first, and 80 kcal mol^{-1} for the second of the two consecutive reactions. In this case, we regard the values arrived at from X-ray data as being more reliable. The method of Kissinger gives much too low a value, even when compared with the results obtained by the method of Piloyan and Coats and Redfern (Table 3). The discrepancy between these values and the ones obtained by X-ray data is readily explained. The reaction is not a simple first-order reaction, as expected from the DTA and TG traces. Instead, it is a consecutive reaction, made up of two first-order reactions. Two reactions with fairly slow reaction rates superimposed on each other yield a picture of one reaction, with a faster reaction rate and thus a lower activation energy. Considering rate equations for simple first-order reactions and consecutive reaction[12], respectively, it is obvious that the results obtained by treating the reaction as an overall first-order simple reaction must be erroneous.

For the third reaction, the value of the activation energy of 30 kcal mol^{-1} calculated from X-ray data falls between the data derived from DTA and TG (22 and 43 kcal mol^{-1}). For the fourth reaction, X-ray data and DTA show excellent agreement; TG data yield a value that is about twice as high. For the fifth reaction (final breakdown), all values are above 100 kcal mol^{-1}; X-ray data indicate 171, DTA 101, TG 128 kcal mol^{-1}. To summarize, it can be stated that estimates of the activation energy seem to be as reliable (or unreliable) as all other conventional methods. However, the method has the advantage that a given reaction can be pin-pointed from both the decomposing and the forming constituent. Furthermore, a detailed study of

consecutive reactions (as well as parallel reactions) can be made, which is not possible with conventional methods. The fact that good agreement can be achieved between independent dynamic methods seems to be verified.

(c) Dependence of E on pressure

Using the method of Piloyan (see above), the activation energies for the first and second reaction indicated on high-pressure DTA traces have been calculated. For the first reaction (15Å → 13.8Å → 11.8Å), the activation energy decreases with pressure (Fig. 4), which can be expressed in the equation $E = 84.117 - 13.390 \ln P$ (coefficient of correlation 0.99).

As the reaction involves the release of a gas phase (water), it should be inhibited by increasing pressure. But, as shown above, the reaction proceeds with a decrease in volume. Thus, the reaction follows Le Chatelier's principle, and proceeds faster the higher the pressure is.

For the second reaction (11.8 → 10.5 → 10.1Å), for pressures of 5 and 100 bars a similar trend is indicated. However, with increasing pressure (100 → 165 → 380 bars) a contradicting trend is noted: the activation energy rises with increasing pressure.

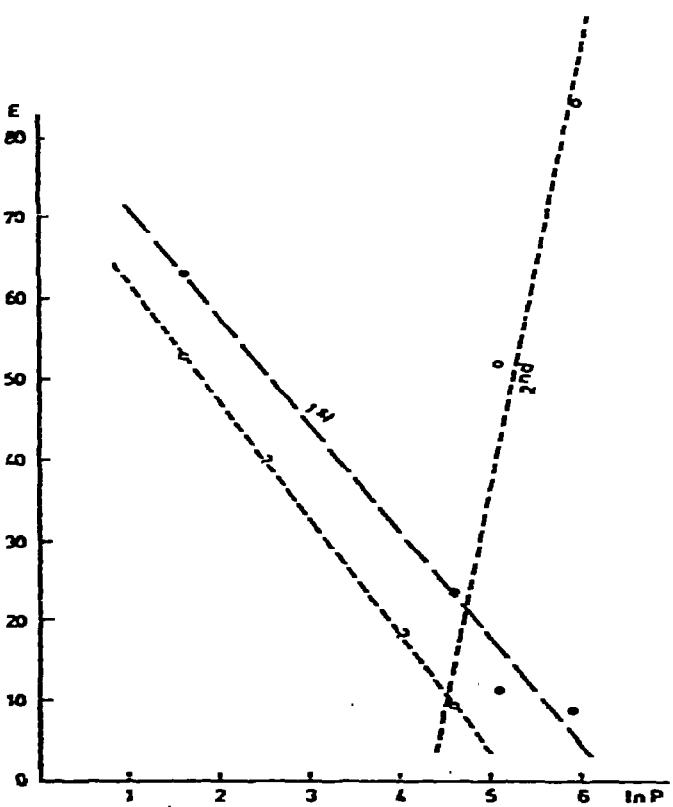

Fig. 4. High-pressure DTA of vermiculite specimen no 3: E versus $\ln P$.

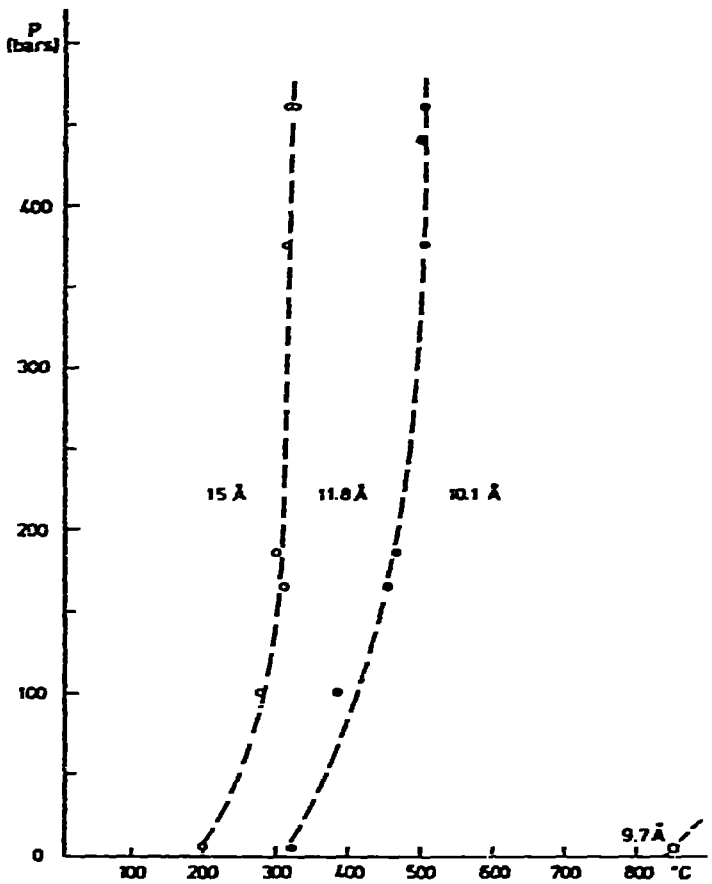

Fig. 5. High-pressure DTA of Sokli vermiculite, specimen No. 3, *P–T* plot.

As this reaction involves expansion of the material, this behaviour can be understood. At present, it is not clear why the reaction at 5 bars pressure deviates from this trend; a different reaction mechanism might be involved.

(d) Enthalpy (ΔH)

The enthalpies of the first two reactions registered by DTA were calculated from high-pressure DTA data. High-pressure DTA was carried out in an argon atmosphere, principally because H_2O pressure, which would have been most realistic from a geological point of view, was not obtainable.

A plot of T_i versus pressure, Fig. 5, shows that the high-temperature phases have higher molar enthalpy and higher molar volume than the low-temperature phases. The value for $\Delta V_{(mol)}$ decreases steadily with increasing pressure, until it approaches zero at pressures above 300 bars, and temperatures in the range 300–400 °C. This is explained by water being in the supercritical state under these conditions (the value of $\Delta V_{(mol)}$ is approximately equal to the amount of water released).

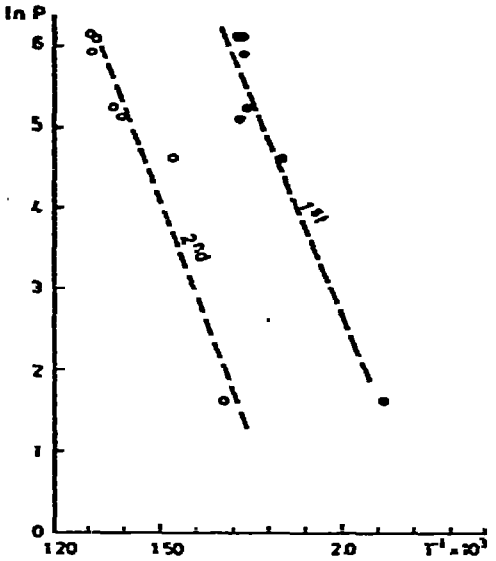

Fig. 6. High-pressure DTA: ln$P$ versus $1/T$. Slope = $\Delta H/R$.

The enthalphy of the reactions can be determined by using the Clausius-Clapeyron equation

$$\frac{dP}{dT} = \frac{\Delta HP}{RT^2}$$

or after integration,

$$\ln P = \frac{\Delta H}{RT} + C$$

Thus, a plot of ln$P$ against $1/T$ will result in a straight line with the slope $\Delta H/R$. The plot, Fig. 6, yields a straight line, even if there are rather few data on the low-pressure side.

Using linear regression analysis, the following values for ΔH have been calculated:

15Å → 13.8Å → 11.8Å, ΔH = 21.3 kcal mol^{-1} (coeff. of correl. 0.98).

11.8Å → 10.5Å → 10.1Å, ΔH = 21.2 kcal mol^{-1} (coeff. of correl. 0.96).

ACKNOWLEDGEMENTS

The authors are grateful to Netzsch GmbH for STA measurements and to Rautaruukki Oy, Finland for supplying the samples.

REFERENCES

1 H. Paarma, *Lithos*, 3 (1970) 129.
2 H. Vartiainen and A. R. Woolley, *Bull. Geol. Soc. Finl.*, 46 (1974) 81.
3 R. C. Mackenzie, *Differential Thermal Analysis*, Vol. 1, Academic Press, London, 1970.
4 I. Barshad, *Am. Mineral.*, 35 (1950) 225.
5 G. F. Walker and W. F. Cole, in R. C. Mackenzie (Ed.), *The Differential Thermal Investigation of Clays*, Min. Soc. London, 1957, p. 191.
6 B. S. Bobrov, Yu. Ye. Gorbatyy and M. B. Epelbaum, *Geochem. Int.*, 7 (1970) 530.
7 G. F. Walker, in G. W. Brindley (Ed.), *X-Ray Identification and Crystal Structures of Clay Minerals*, Min. Soc. London, 1951, p. 199.
8 G. Gyulai and E. S. Greenhow, *Thermochim. Acta*, 7 (1973) 254.
9 H. E. Kissinger, *Anal. Chem.*, 29 (1957) 1702.
10 G. O. Piloyan, I. D. Ryabchikov and O. S. Novikova, *Nature*, 5067 (1966) 1229.
11 A. W. Coats and S. P. Redfern, *Nature*, 201 (1964) 68.
12 J. Šesták, V. Šatava and W. W. Wendlandt, *Thermochim. Acta*, 7 (1973) 333.